

Dendrimers of Nanometer Size Based on Metal Complexes: Luminescent and Redox-Active Polynuclear Metal Complexes Containing up to Twenty-Two Metal Centers

Sebastiano Campagna,* Gianfranco Denti,* Scolastica Serroni, Alberto Juris, Margherita Venturi, Vittorio Ricevuto, and Vincenzo Balzani*

Abstract: Treelike (dendritic) structures made of Ru^{II}-polypyridine complexes have been prepared by the "complexes-as-metals and complexes-as-ligands" synthetic strategy. The key building blocks are Ru^{II} complexes of the 2,3-bis-(2-pyridyl)pyrazine (2,3-dpp) bridging ligand, where one of the two chelating sites can be protected by methylation. Dendrimers containing four, ten, and twenty-two metal ions have been obtained. These

dendrimers exhibit strong absorption in the UV/Vis spectral region, a moderately strong red luminescence, and a great number of metal-based oxidation and ligand-

based reduction processes. The nature of the terminal ligands determines in which subunits of the supramolecular array the HOMO and LUMO orbitals and the luminescent excited state are localized. The reported synthetic strategy is efficient, characterized by a full, step-by-step control of the growth process, and can be easily extended to building blocks containing other metals and/or ligands.

Keywords

dendrimers · luminescence · molecular devices · ruthenium complexes · redox systems

Introduction

Much attention is currently devoted^[1] to the preparation of highly branched treelike species, variously called cascade molecules,^[2] arborols,^[3] or dendrimers.^[4] The reasons why such compounds are interesting from a fundamental viewpoint and promising for a variety of applications have been reviewed^[5] and highlighted^[6] by several authors. Of particular interest are treelike structures (dendrimers) that incorporate specific "pieces of information" in their building blocks such as the capability to absorb and emit visible light and to reversibly exchange electrons.^[7] Such species, in fact, could find applications as components in molecular electronics^[8] and as photochemical molecular devices^[9] for solar energy conversion and information storage.^[9–12] Polypyridine transition metal complexes are ideal components to build up dendrimers of this type.^[13] We have developed a divergent synthetic procedure based on the "complexes-as-metals and complexes-as-ligands" strategy^[7] to prepare luminescent and redox-active dendrimers where the desired metals and ligands can be placed in specific sites of the

supramolecular structure. Species containing four,^[14, 15] six,^[16] seven,^[17] ten,^[18] and thirteen^[19] metal-based units have already been described. Dendrimers containing metal atoms have also been reported by other groups.^[20] In this paper we illustrate a generalized version of the synthetic strategy, based on an iterative protection/deprotection procedure. In principle, this divergent strategy can be used to prepare compounds of even higher nuclearity. We also describe the absorption, luminescence, and redox properties of three mononuclear building blocks, six intermediate species with four and ten metal centers (which represent the first and second generation, respectively, of our dendrimers), and a third generation compound, which contains twenty-two metal centers.^[21]

Results and Discussion

Metal and ligands: The reasons for the choice of Ru^{II} as a metal, 2,3-bis(2-pyridyl)pyrazine (2,3-dpp) as a bridging ligand, and 2,2'-bipyridine (bpy) as terminal ligand (Fig. 1) have been discussed elsewhere.^[7a, 7d, 18b] Essentially, these ligands can be easily coordinated to Ru^{II} to give stable metal complexes, which exhibit intense absorption bands in the UV and visible spectral region, a reasonably strong and long-lived luminescence, and an extremely rich redox behavior^[13] (reversible one-electron oxidation at the metal center and reversible multielectron reduction at each ligand).^[22] A particular important point is that 2,3-dpp can be easily methylated, so that one of the two chelating sites can be protected from coordination.^[23] The methylated form of 2,3-dpp, 2,3-Medpp⁺, is also shown in Figure 1.

[*] S. Campagna, V. Ricevuto, S. Serroni
Dipartimento di Chimica Inorganica e Struttura Molecolare
Università di Messina
98166 Villa S. Agata, Messina (Italy)
G. Denti
Laboratorio di Chimica Inorganica, Istituto di Chimica Agraria
Università di Pisa, 56124 Pisa (Italy)
V. Balzani, A. Juris, M. Venturi
Dipartimento di Chimica "G. Ciamician"
Università di Bologna, 40126 Bologna (Italy)

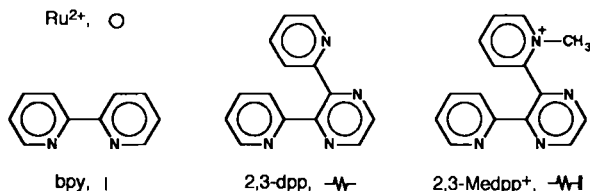
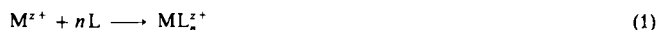


Fig. 1. Formulas of the ligands, and abbreviations and symbols used to represent the components of the dendrimers.

“Complexes-as-metals and complexes-as-ligands” synthetic strategy: Mononuclear transition metal complexes are synthesized by combining metal ion (M^{z+}) and free ligands (L), as shown in Equation (1). In the last few years we and others have



been developing a procedure to synthesize polynuclear metal complexes of desired nuclearity and chemical structure.^[7, 15, 22a–c] Such a procedure is based on the use of *complexes* (building blocks) in the place of the metal ion (M^{z+}) and/or of the ligands (L) in Equation (1). The place of M^{z+} can be taken by mono- or oligonuclear complexes that possess labile ligands, so that they can give rise to species with unsaturated metal coordination sites (“complex metals”), and L can be replaced by mono- or oligonuclear complexes that contain free chelating sites (“complex ligands”).

Building blocks: The compounds described in this paper are schematized in Figure 2. Each compound is designated by a label where the number indicates the nuclearity, the letter whether the peripheral ligands are deprotected (d) or protected

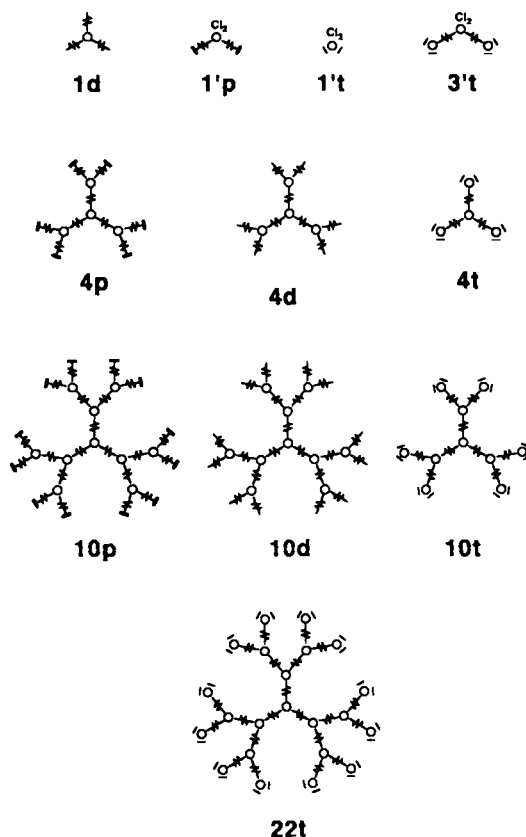


Fig. 2. Schematic representation of the compounds used for and/or obtained by our synthetic strategy (for symbols used to represent metal and ligands, see Fig. 1; for explanation of compound labels, see text).

(p) bridging ligands, or terminal (t) monochelating ligands, and the “prime” notation the presence of labile ligands (Cl^-). Figure 3 shows a more conventional representation of compound 10t.

The two key compounds for the synthesis of our dendrimers are the mononuclear $[Ru(2,3-dpp)_3]^{2+}$ (1d) and $[Ru(2,3-Medpp)_2Cl_2]^{2+}$ (1'p) species. Compound 1d, first prepared by Petersen et al.,^[24] is a “complex ligand” since it contains three



Editorial Board Member:^[*] Vincenzo Balzani received his “laurea” in Chemistry at the University of Bologna in 1960. Since 1972 he has been a Professor of Chemistry at the same University. He was Director of the FRAE-CNR institute of Bologna (1977–1988) and Chairman of the European Photochemistry Association (1988–1992). He has obtained several awards, including the Canizzaro Gold Medal of the Italian Chemical Society (1988), the Doc-

torate Honoris Causa from the University of Fribourg, Switzerland (1989), the Ziegler–Natta Lectureship of the Gesellschaft Deutscher Chemiker (1994), and the Italgas European Prize for Research and Innovation (1994). His research interests include supramolecular chemistry, photochemistry, photophysics, electron- and energy-transfer processes, photo-, chemi- and electrochemiluminescence, photocatalysis, and photochemical molecular devices. He has published more than 280 scientific papers, is the editor of two books, and is the author of two monographs: *Photochemistry of Coordination Compounds* (with V. Carassiti), Academic Press, London, 1970, and *Supramolecular Photochemistry* (with F. Scandola), Horwood, Chichester, 1991.

[*] Members of the Editorial Board will be introduced to the readers with their first manuscript.

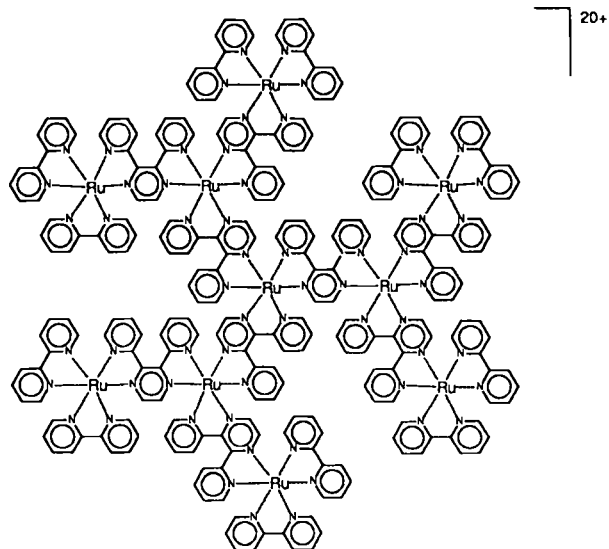


Fig. 3. Representation of 10t complex showing all bonds.

vacant chelating sites. As we will see later, this species plays the role of a “core” in the synthesis of our dendrimers. Compound **1'p** is an extremely interesting species prepared in our laboratories. It contains two labile Cl^- ions, and therefore can play the role of a “complex metal”. Furthermore, once it has been used as a “complex metal”, its two methylated ligands can be deprotected, and the new compound can thus be used as a “complex ligand”. The building blocks $[\text{Ru}(\text{bpy})_2\text{Cl}_2]$ (**1't**) and $[\{\text{Ru}(\text{bpy})_2(\mu\text{-}2,3\text{-dpp})\}_2\text{RuCl}_2]^{4+}$ (**3't**), which contain terminal bpy ligands, can only play the role of “complex metal” and, as we will see below, they can be used “to close” the structure of a dendrimer (termination steps), that is, to obtain a species that cannot be further expanded (“sterile” species). The use in the termination steps of a “t-type compound” containing different metals and/or terminal ligands can lead to a variety of mixed-metal and/or mixed-ligand compounds (see below).

Protection and deprotection: A divergent synthetic approach to polynuclear polypyridine complexes must be necessarily based on synthons such as $[\text{Ru}(2,3\text{-dpp})_2\text{Cl}_2]$, which is at the same time a “complex ligand” and a “complex metal”. In order to obtain a reasonable yield of synthons belonging to the “complex ligand” class, one needs a method capable of forcing a potentially bischelating ligand to act as a monochelating one. A possibility is the in situ protonation of the pyridyl nitrogens that are to be inactivated toward coordination. This method, however, does not preclude formation of unwanted compounds of various nuclearities.^[17] Therefore we have elaborated a procedure to methylate 2,3-dpp^[23] at one pyridyl nitrogen by using trimethyloxonium tetrafluoroborate or methyl triflate (methyl trifluoromethanesulfonate) as alkylating agents. The resulting protected ligand 2,3-Medpp⁺ (Fig. 1) allowed the facile, high-yield (90%) preparation of synthon $[\text{Ru}(2,3\text{-Medpp})_2\text{Cl}_2]^{2+}$ (**1'p**); the protection proved to be stable under the conditions employed for the successive reactions of **1'p** as a “complex metal”, and we were able to set up a deprotection procedure fully compatible with the stability of the metal–ligand bonds (see Experimental Section).

Synthesis of the dendrimers: The divergent synthetic approach is shown in Figure 4. Reaction of the “complex ligand” **1d** with the “complex metal” **1'p** in a 1:3 molecular ratio led to the tetranuclear complex **4p** (first generation of our dendrimers), which contains six protected chelating sites in its periphery. Demethylation of **4p** yields the tetranuclear complex **4d**, which can play the role of “complex ligand”. Reaction of **4d** with the “complex metal” **1'p** in 1:6 molecular ratio yielded the decanuclear compound **10p** (second generation of our dendrimers). Deprotection of **10p** led to the decanuclear “complex ligand” **10d**, which contains 12 vacant chelating sites. The divergent iterative synthesis has been carried out up to this stage. In principle, iteration of this procedure can lead to further generations, but difficulties are to be expected due to the increasing number of reaction sites.^[15] The reaction of the “complex ligand” deprotected species (**d**-family) with “complex metals” building blocks (“t”-family, e.g., **1't** and **3't**) yields coordinatively saturated (sterile) dendrimers (termination steps, Fig. 4). We had previously carried out the reaction of **1d**-type with **3't**-type compounds to obtain a variety of decanuclear complexes.^[18] Now we have reacted **4d** with **3't** (Fig. 5) to yield the third generation docosanuclear complex **22t**.^[17b, 25] This compound was reasonably well characterized with different techniques (see below). To our knowledge, **22t** (Fig. 6) is one of the largest Werner-type transition metal complexes obtained so far. Dendrimers containing

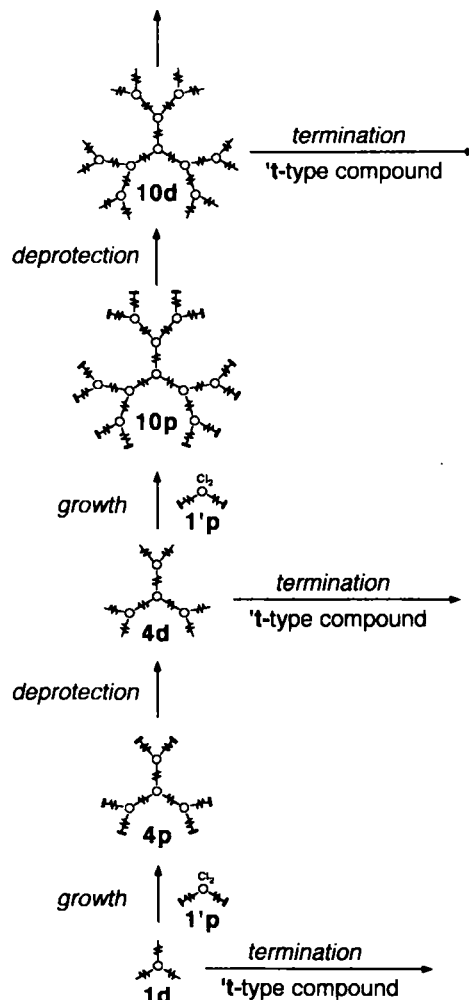


Fig. 4. Divergent synthetic strategy for the preparation of dendrimers based on transition metal complexes (symbols are explained in Figs. 1 and 2). The termination steps yield sterile dendrimers and may be used for the synthesis of mixed-metal and/or mixed-ligand compounds, as shown in Figure 13.

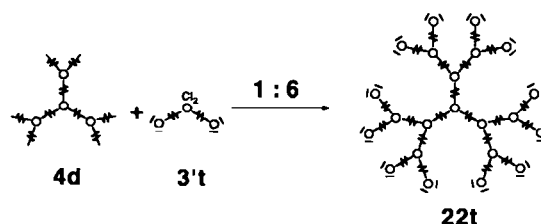


Fig. 5. Synthetic scheme for the preparation of complex **22t**.

12 Ru^{2+} ions or 24 Co^{2+} ions have been reported by Newkome et al.^[20a, d] Not counting the 44 PF_6^- counterions, the **22t** species is made of 1090 atoms, has a molecular weight of 10 890 daltons, and an estimated size of 5 nm. Besides the 22 Ru^{II} metal atoms, it contains 24 terminal bpy ligands and 21 2,3-dpp bridging ligands.

Characterization of the dendrimers: Characterization of large molecules like dendrimers is a difficult task.^[15] For neutral compounds, techniques based on colligative properties can be used to determine the molecular mass. Our compounds, however, are highly charged ions, and the use of the above techniques is not advisable because of the high number of counterions. Mass

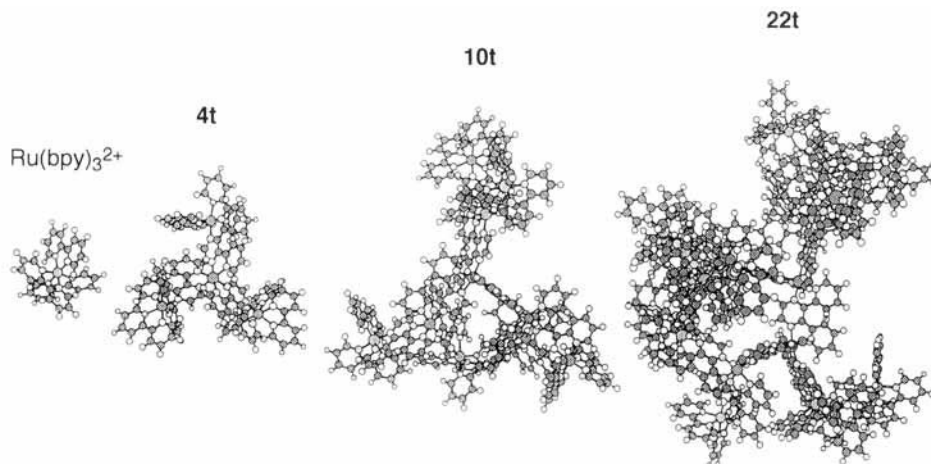


Fig. 6. Computer models of $[\text{Ru}(\text{bpy})_3]^{2+}$, **4t**, **10t**, and **22t** complexes.

spectrometry has not yet been developed for compounds carrying such a high electric charge, and light scattering can hardly be used because of the strong absorption in all the UV and visible spectral region.

In spite of the above difficulties, a reliable characterization of our dendrimers has been achieved by using a variety of techniques:

1) Each compound (including precursors) was purified until TLC showed the presence of only one spot.

2) Each building block was checked to be stable under the experimental conditions. It is already known that in such compounds no ligand or metal scrambling occurs, as shown by the synthesis of a number of tetra-^[14d], hexa-^[16] and decanuclear^[18] species containing different metals and/or ligands in predetermined sites of the structure.

3) Each one of the three types of steps (growth, deprotection, termination; Fig. 4) were accurately monitored as follows:

Growth steps: i) The reaction of the "complex ligand" (**d**-family) compounds with the "complex metal" **1'p** was carried out under stoichiometric conditions. TLC analysis (Al_2O_3 , $\text{CH}_2\text{Cl}_2/\text{MeOH}$ 9:1) showed that in each case at least 90% of **1'p** had reacted. ii) For the product of the **p**-family obtained in each growth step the ratio of aromatic to aliphatic protons in the ^1H NMR spectrum (where the strong signals of the methyl protons lie in a clean spectral window around $\delta = 4$) was consistent with the expected formulations. iii) IR analysis on the **p**-family products showed the absence of the 990 cm^{-1} band of unbridged 2,3-dpp.

Deprotection steps were carried out with a large excess of demethylating agent. The purified products did not show any ^1H NMR signal corresponding to methyl groups, so we can exclude the presence of residual methylated sites (< 1%).

Termination steps: The reaction of the complexes of the **d**-family with the "complex metal" **3't** (which was fully characterized by several techniques including FAB MS)^[18b, 26] was carried out under stoichiometric conditions until complete (> 90%) disappearance of **3't** (TLC analysis). Methylation of the **t**-family products was not observed under conditions that result in complete methylation of $[\text{Ru}(\text{bpy})_2(2,3\text{-dpp})]^{2+}$ (see Experimental Section); this demonstrated the absence of free chelating sites in the former (easily checked by ^1H NMR) and shows that the termination step had gone to completion (3% uncertainty).

4) As we will show below, the luminescence and electrochemical properties are fully consistent with the reported formulations.

General properties: All the compounds dealt with in this paper (Fig. 2) are soluble in common solvents (e.g., CH_2Cl_2 , CH_3CN) and are stable both in the dark and under light excitation. In principle, they can exist as different isomers, depending on the arrangement of the ligands around the metal ions. A 2D-COSY ^1H NMR spectrum (400 MHz) of the $[\text{Ru}(2,3\text{-dpp})_3]^{2+}$ "core" (**1d**) shows that the purified material is a mixture of the *mer* and *fac* isomers in which the *mer* isomer predominates (92%).^[27] The poly-metallic complexes can also be a mixture of several diastereoisomeric species, since each metal center is a stereogenic center. For these reasons

structural investigations on these systems are difficult. Differences in the electrochemical and spectroscopic properties described below arising from the presence of isomeric species are not expected to be large.^[28]

As can be seen from the schematic views shown in Figures 2, 3, and 6, the species with high nuclearity exhibit a three-dimensional branching structure of the type observed in otherwise completely different dendrimers based on organic components.^[11–6] Therefore, *endo*- and *exo*-receptor properties^[15] can be expected, which will be the object of future investigations. We would like to stress that our dendrimers differ from most of those prepared so far for two fundamental reasons: 1) each metal-containing unit exhibits valuable intrinsic properties such as absorption of visible (solar) light, luminescence, and oxidation and reduction levels at accessible potentials;^[13] and 2) by a suitable choice of the building blocks, different metals and/or ligands can be placed in specific sites of the supramolecular array, as we have already shown for the tetra-^[14] hexa-^[16] and decanuclear^[18] species (see below). In other words, our dendrimers are species that can incorporate many "pieces of information" and therefore can be used to perform valuable functions such as light harvesting, directional energy transfer, and exchange of a controlled number of electrons at a given potential.^[7c–f, 14b, c, 16b, 18b, 29]

The ligands involved in our dendrimers exhibit different electron donor and acceptor properties. From the electrochemical^[22f, 29a] and luminescence^[29a] behavior of the complexes of the $[\text{Ru}(\text{bpy})_n(2,3\text{-dpp})_{3-n}]^{2+}$ family, it can be deduced that bpy is a better electron-donor ligand than 2,3-dpp, and that monochelated 2,3-dpp is easier to reduce than coordinated bpy. When 2,3-dpp plays the role of a bis-chelated bridging ligand, its electron donating power toward a single metal decreases, because the pyrazine ring is involved in the coordination of both metal ions. Furthermore, its reduction potential becomes more positive by about 0.4 V.^[29a] Methylation of 2,3-dpp mainly affects one of the pyridine rings. Therefore the electron-donor and -acceptor properties of the other chelating site are only slightly affected, but a new easily reducible center (the methylated pyridine ring) is now present. The latter center is likely to contain the LUMO orbital of the complex. In the dendritic species each metal-based unit will bring its own excited state and redox properties. It should be pointed out, however, that these properties are affected by intercomponent interaction (see below).

Electrochemical behavior: Previous investigations on oligonuclear complexes of the 2,3-dpp family containing the terminal

ligand bpy have shown that^[14–19, 22, 29] 1) oxidation is metal-centered; 2) reduction is ligand-centered; 3) the 2,3-dpp bridging ligands are reduced at less negative potentials than the terminal bpy ligands; and 4) metal–metal and ligand–ligand interactions are noticeable for metals coordinated to the same bridging ligand and for ligands coordinated to the same metal, whereas they are small for metals or ligands that are sufficiently far apart.

The $E_{1/2}$ values (V vs. SCE) of the observed redox waves for the examined compounds are collected in Table 1. In the case of oxidation, the observed waves are reversible with $\Delta E \approx 60$ mV except for multielectron waves where ΔE can reach 120 mV. For reduction, the criteria for reversibility (see Experimental Section) are difficult to apply because of waves overlapping (especially in the case of waves involving different numbers of electrons).

Table 1. Electrochemical results in argon-purged acetonitrile solution at room temperature [a].

| | $E_{1/2}^{\text{ox}} [n] [b]$ | $E_{1/2}^{\text{red}} [n] [b]$ |
|------------------------------------|---------------------------------|--------------------------------------------|
| $\text{Ru}(\text{bpy})_3^{3+} [c]$ | +1.29 [1] | –1.33 [1]; –1.52 [1]; –1.78 [1] |
| 1d [d] | +1.60 [1] | –0.94 [1]; –1.12 [1]; –1.40 [1] |
| 1p | +0.66 [1] [e] | –0.78 <i>irr</i> [1]; –0.93 <i>irr</i> [1] |
| 1't [f] | +0.32 [1] | –1.67 <i>irr</i> ; –1.78 <i>irr</i> |
| 4d | [g] | [g] |
| 4p | +1.82 [1] [e] | –0.79 <i>irr</i> [6]; –0.98 <i>qr</i> [3] |
| 4t [h] | +1.53 [3] | –0.62 [1]; –0.77 [1]; –1.23 [1] |
| 10d | $\approx +1.69 [\approx 6] [g]$ | [g] |
| 10p | +1.83 [3] | –0.75 <i>irr</i> [12]; –0.94 <i>qr</i> [3] |
| 10t | +1.53 [6] [i] | –0.73 [6]; –1.22 [3] |
| 22t | +1.52 [12] | [j] |

[a] Potentials in volts vs. SCE; unless otherwise noted, the waves are reversible; *qr* = quasi-reversible (see text); *irr* = irreversible; for *qr* and *irr* reductions, the potential is evaluated from the DPV peaks; for the symbols used to indicate the compounds, see Figure 2. [b] Number of electrons exchanged in square brackets. [c] This work; data in agreement with previously reported values, see ref. [13a]. [d] For previously reported data, see ref. [24] (E^{ox} reported as +1.68 V). [e] Revised values; for previously reported data see ref. [7b]. [f] B. P. Sullivan, D. J. Salmon, T. J. Meyer, J. Peedin, *Inorg. Chem.* **1979**, *18*, 3369. [g] Adsorption on the electrode. [h] Revised values; for previously reported data, see refs. [14b] and [15]. [i] Revised values; for previously reported data, see ref. [18b]. [j] See text.

Electrochemical oxidation: For the mononuclear species, the relatively low potential for the oxidation of **1't** and **1p** compared to that of $[\text{Ru}(\text{bpy})_3]^{2+}$ (which in our shorthand notation would be **1t**) can be attributed to the presence of the Cl^- ligands. The potential for the oxidation of **1d** (Table 1) is more positive than that of $[\text{Ru}(\text{bpy})_3]^{2+}$, because, as mentioned above, 2,3-dpp is a weaker electron donor than bpy. Preliminary results show that $[\text{Ru}(2,3\text{-Medpp})_3]^{5+}$ (**1p**) is even more difficult to oxidize.

For the tetranuclear compound **4d** meaningful results cannot be obtained because it adsorbs strongly on the electrode. Compound **4t** (Fig. 7) exhibits a three-electron oxidation wave; this indicates that the three equivalent peripheral units are oxidized at nearly the same potential. However, **4p** (Fig. 7) exhibits a one-electron oxidation wave, at a much higher positive potential (Table 1). This shows that 1) in **4p** the central metal ion is easier to oxidize than the peripheral ones, and 2) the peripheral $[\text{Ru}(2,3\text{-Medpp})_2]^{4+}$ units are much more difficult to oxidize than the peripheral $[\text{Ru}(\text{bpy})_2]^{2+}$ units. Furthermore, comparison of the potentials for the oxidation of **1d** and **4p** shows that coordination of $[\text{Ru}(2,3\text{-Medpp})_2]^{4+}$ units considerably increases the potential for the oxidation of the **1d** core.

Complex **10t** (Fig. 8) exhibits a six-electron oxidation wave that can be attributed to the oxidation, at nearly the same poten-

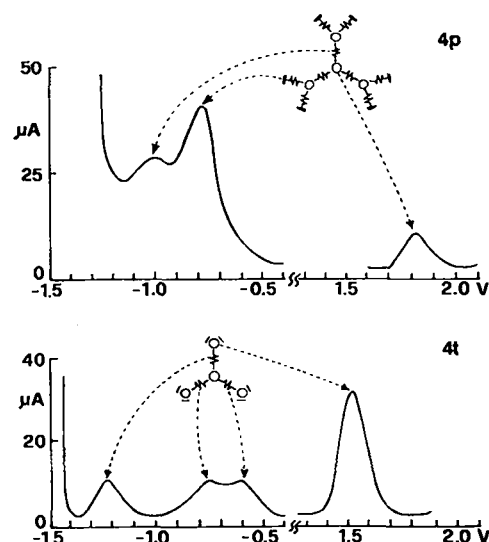


Fig. 7. Differential pulse voltammetry of **4t** and **4p** complexes (platinum working electrode).

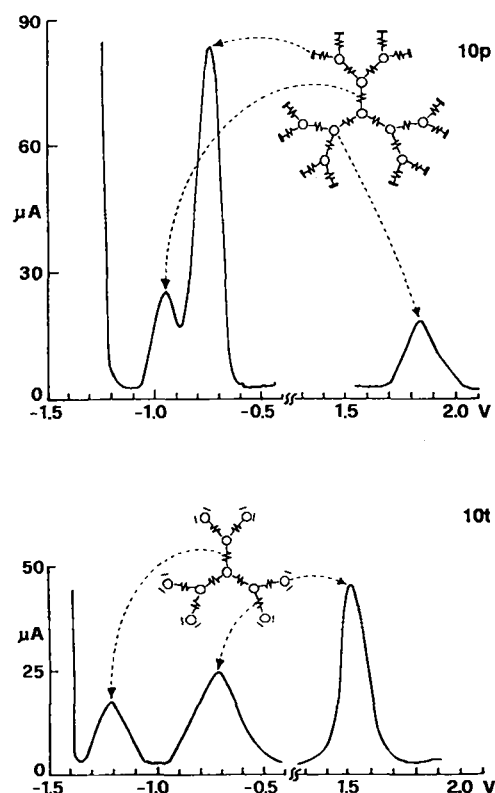


Fig. 8. Differential pulse voltammetry of **10t** and **10p** complexes (platinum working electrode).

tial, of the six equivalent peripheral metal ions.^[18b] To a first approximation, the potential for the oxidation of the central and intermediate metal ions should be similar to that of the central metal ion of **4p** (+1.82 V). After oxidation of the peripheral units, the oxidation of the central and intermediate units will of course be displaced to more positive potentials. To evaluate the extent of this displacement for the central metal, one can use a correlation with the analogous Os complexes,^[18b] where the potential for the oxidation of the central metal ion is displaced by 0.22 V when the six peripheral units are oxidized. Therefore,

the oxidation of the central Ru ion of **10t** after oxidation of the peripheral units should be around $(1.82 + 0.22)$ V, that is, near the end of the potential window examined. Oxidation of the intermediate units would of course occur at even more positive potentials, because of the interaction with the nearby oxidized peripheral units.

For compound **10d** adsorption on the electrode makes the data relatively unreliable. It seems, again, that the oxidation occurs at the peripheral metal ions. The potential at which oxidation takes place is more positive than that observed in the case of **10t** because the ligand 2,3-dpp is a weaker donor than bpy. The agreement with the potential for the oxidation of **1d** is satisfactory.

For compound **10p** a three-electron oxidation wave is observed, suggesting that the oxidation involves the three equivalent intermediate metal ions.^[30] As can be seen from Figure 8, the differential pulse voltammetry (DPV) peak is somewhat broader than that of **10t**. The oxidation of the six peripheral units in **10p** is displaced to more positive potentials by the presence of the positive charge on the 2,3-Medpp⁺ terminal ligands. The potential at which oxidation takes place is more positive than in the case of **10t** and **10d** because inner metal ions are involved.

In agreement with the behavior shown by **10t**, the oxidation of **22t** involves the peripheral metal ions, which are equivalent as indicated by the presence of a twelve-electron oxidation wave. For **10t** and **22t** the oxidation takes place at practically the same potential because, in the two complexes, the peripheral metal ions involved in the process are in the same "surrounding" conditions. On the basis of the above discussion, oxidation of the inner metal ions in **22t** (not directly connected to the oxidized ones) should occur around + 2.0 V. As for **10t**, no successive oxidation can be observed, presumably because of the large positive charge accumulated in the periphery.

Electrochemical reduction: Because of the presence of a large number of polypyridine ligands, each capable of undergoing several reduction processes,^[2,2f] the electrochemical reduction of the examined compounds shows very complex patterns. Compounds **4d** and **10d** are adsorbed on the electrode and do not give reliable results.

The first reduction wave of compound **1d** (Table 1) occurs at -0.94 V, in agreement with the value reported in ref. [24], and corresponds to a one-electron process. Comparison with the value for $[\text{Ru}(\text{bpy})_3]^{2+}$ shows that, as mentioned above, coordinated 2,3-dpp is much easier to reduce than coordinated bpy. Comparison with the value for **1p** (-0.80 V) shows that methylation displaces the reduction potentials toward positive values. Comparison between **1't** and $[\text{Ru}(\text{bpy})_3]^{2+}$ (Table 1) shows that the presence of two Cl^- ions moves the reduction potentials to more negative values. It should also be noted that the first reduction wave of **1'p** is not displaced to more negative potentials with respect to that of **1p**, despite the presence of two Cl^- ions. This indicates that reduction of the protected ligands takes place in the external methylated sites.

As far as the tetranuclear complexes are concerned (Fig. 7), compound **4t** exhibits three one-electron reduction waves starting at -0.62 V, which can be attributed to successive reduction of interacting bridging ligands. For potentials ≤ -1.4 V other overlapping waves are present (not shown in Fig. 7) that can be attributed to the second reduction of the bridging ligands followed by the reduction of the bpy ligands. Compound **4p** shows a six-electron wave at -0.79 V, which can be assigned to the one-electron reduction of the six methylated peripheral ligands at nearly the same potential. A broad wave involving three

electrons follows at more negative potential, assigned to reduction of the three bridging ligands. For potentials ≤ -1.2 V unresolved waves are observed (not shown in Fig. 7), which could represent the second reduction of the methylated ligands followed by the second reduction of the bridging ligands.

Compound **10t** (Fig. 8) shows two broad waves (at -0.73 and -1.22 V) followed by several other overlapping waves. The first wave, which corresponds to six-electron reduction process, may be attributed to the one-electron reduction of the six outer equivalent bridging ligands. Since the six processes take place at approximately the same potential, the six ligands interact only slightly with one another. This would suggest that the LUMO orbital mainly involves the more external chelating site of the 2,3-dpp bridging ligand. The second wave, which involves three electrons, should represent the one-electron reduction of the three inner bridging ligands, again mainly on their external chelating site. The several overlapping waves present in the voltammograms at more negative potentials (not shown in Fig. 8) should correspond to the second reduction of the bridging ligands followed by the reduction of the bpy ligands.

In compound **10p** (Fig. 8) two waves are present (-0.75 and -0.94 V), followed by several other overlapping waves. The first wave, which involves a twelve-electron reduction process, corresponds to the one-electron reduction of the twelve outer methylated ligands. The second wave, which involves a three-electron reduction process, can be assigned to the one-electron reduction of the three inner bridging ligands. The six intermediate bridging ligands, because of their closeness to the already reduced outer ligands, can be reduced only at more negative potential than the three inner ligands. This is also in agreement with the fact that the reduction of the inner bridging ligands in **10p** takes place at a potential less negative than in **10t**, where the inner ligands are close to the already reduced six intermediate ligands. The unresolved waves observed at potentials ≤ -1.1 V (not shown in Fig. 8) should correspond to the reduction of the six intermediate bridging ligands overlapping the second reduction of the methylated ligands. For **22t**, both the CV and DPV patterns show the presence of many overlapping waves that can hardly be assigned.

It is instructive to see how the reduction potentials of the three 2,3-dpp ligands of the central core change on going from the mononuclear **1d** to the tetra- and decanuclear complexes (Fig. 9). In **1d** the three ligands are reduced at different potentials; this shows that there is a noticeable ligand–ligand interaction through the central metal. In **4t** the three processes are still well separated, but they occur at less negative potentials, because the LUMO of each bridging ligand is stabilized by $[\text{Ru}(\text{bpy})_2]^{2+}$ coordination. For **4p**, **10p**, and **10t**, reduction of

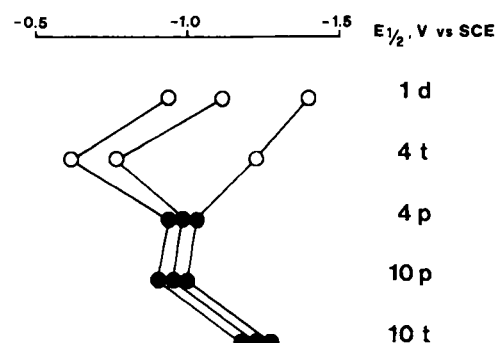


Fig. 9. Correlation between the reduction potentials of the core 2,3-dpp ligands in various complexes. The black circles indicate that the reduction of the core ligand occurs after reduction of other sites (see text).

the central bridging ligands occurs after reduction of other sites (Table 1, Figs. 7 and 8). Under such conditions, the three reduction waves almost coalesce; this indicates that the ligand–ligand interaction through the central metal decreases. A determinant factor for such through-metal interaction is the energy difference between the π^* LUMO of the ligands and the π t_{2g} orbitals of the metal. The decrease in the ligand–ligand interaction could then be explained by the fact that an increase in the LUMO energy of the central bridging ligands caused by the reduction of external units increases the energy difference between ligand LUMO and metal t_{2g} orbitals.

Reduction of the central bridging ligand in **4p** occurs at more negative potentials than in **10p**, because the already reduced sites are closer in the former compound. At first sight it may appear strange that the reduction of the central bridging ligands of **10t** occurs at approximately the same potential as the third reduction of **4t**, in spite of the presence of six outer reduced sites in the former compound. One should consider, however, that in **4t** the third wave is displaced to negative potentials by the ligand–ligand interaction, which is strongly reduced in **10t** (see above).

Absorption and emission properties: Each mononuclear Ru-based unit exhibits intense ligand-centered (LC) bands in the UV region and moderately intense metal-to-ligand charge transfer (MLCT) bands in the visible. As is shown by the electro-

chemical behavior (see above), there is some interaction between the neighboring metal-based units in the polynuclear species. To a first approximation, however, each building block carries its own absorption properties in the polynuclear species, so that the molar absorption coefficients exhibited by the compounds of higher nuclearity are huge (Table 2). The absorption spectra of **10p**, **10d**, **10t**, and **22t** are shown in Figures 10 and 11. The emission spectra of **10p**, **10d**, **10t**, and **22t** are shown in Figures 12 and 11.

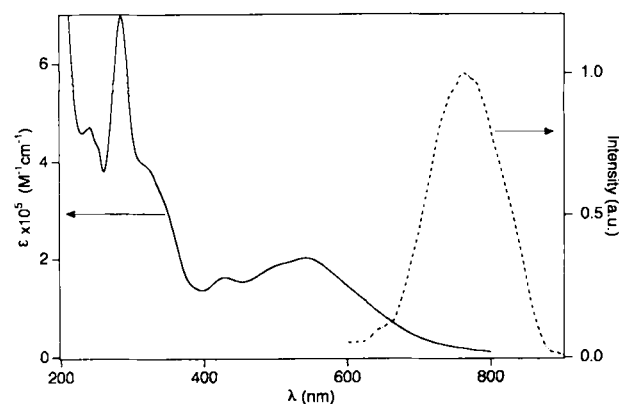


Fig. 11. Absorption (solid line) and luminescence (dashed line) spectra of compound **22t** in acetonitrile solution at room temperature.

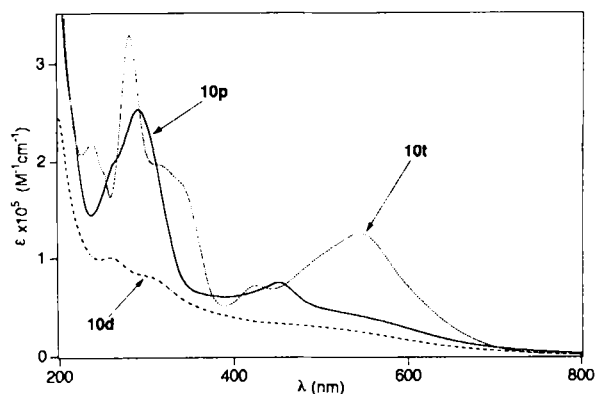


Fig. 10. Absorption spectra of compounds **10p**, **10d**, and **10t** in acetonitrile solution at room temperature.

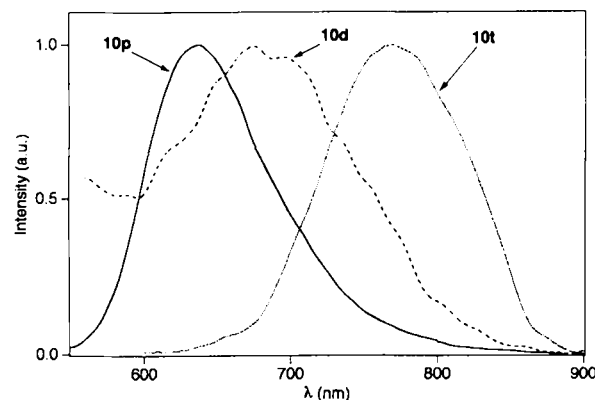


Fig. 12. Luminescence spectra of compounds **10p**, **10d**, and **10t** in acetonitrile solution at room temperature.

Table 2. Spectroscopic and photophysical data [a].

| | Absorption [b] | Luminescence | | | | |
|----------------------------------------|--------------------------------------------------------------------------------------|--------------------------------------|-------------------------------|------------------------|--------------------------------------------------|--------------------|
| | 298 K $\lambda_{\text{max}}/\text{nm}$ ($\epsilon/\text{M}^{-1}\text{cm}^{-1}$) | $\lambda_{\text{max}}/\text{nm}$ [d] | 298 K τ/ns [e] | Φ_{em} [c] | 77 K [c] $\lambda_{\text{max}}/\text{nm}$ [d] | $\tau/\mu\text{s}$ |
| Ru(bpy) ₃ ²⁺ [f] | 452 (13 000), 285 (77 000) | 615 [g] | 1100 | 0.059 [h] | 582 [g] | 5.0 |
| 1 d [i] | 455 (13 000), 281 (52 300) | 623 | 180 [j] | – | 600 | 5.1 |
| 1' p [k] | 663 (4020), 304 (26 900) | – | – | – | – | – |
| 1' t [l] | 538 (9 890) | – | – | – | 752 | 0.17 |
| 4 d [k] | 461 (38 200), 264 (108 000) | 722 | 300 | 1.8×10^{-4} | 698 | 3.6 |
| 4 p [k] | 505 sh (38 000), 296 (137 000) | 714 | 600 | 6.5×10^{-3} | 698 | 4.3 |
| 4 t [m] | 545 (46 000), 285 (149 000) | 811 | 60 | 1×10^{-3} | 727 | 1.4 |
| 10 d | 500 sh (30 000), 260 (101 000) | 750 | [n] | $< 3 \times 10^{-5}$ | [n] | [n] |
| 10 p | 550 sh (40 000), 292 (254 000) | 668 | 600 | 3.9×10^{-4} | 649 | 5.1 |
| 10 t [o] | 541 (125 000), 282 (329 000) | 809 | 55 | 1.0×10^{-3} | 725 | 1.3 |
| 22 t | 542 (202 000), 284 (682 000) | 786 | 45 | 3.0×10^{-4} | 730 | 1.4 |

[a] In acetonitrile solution, unless otherwise noted. [b] Lowest energy band in the visible and prominent absorption maxima in the UV region. [c] In 4:1 MeOH/EtOH matrix. [d] Corrected emission maxima, unless otherwise noted. [e] Deaerated solution. [f] A. Juris, V. Balzani, P. Belser, A. von Zelewsky, *Helv. Chim. Acta* **1981**, *64*, 2175, unless otherwise noted. [g] Uncorrected emission maximum. [h] K. Nakamaru, *Bull. Chem. Soc. Jpn.* **1982**, *55*, 1639. [i] For previously reported data, see ref. [25]. [j] Aerated solution. [k] For preliminary data see ref. [7b]. [l] In *N*-methylformamide solution: P. Belser, A. von Zelewsky, A. Juris, F. Barigelli, V. Balzani, *Gazz. Chim. Ital.* **1983**, *113*, 731. [m] Refs. [14b] and [15]. [n] Emission intensity too weak. [o] Ref. [18b].

Compounds **4t**, **10t**, and **22t** are "sterile" dendrimers of the same **t**-family (first, second, and third generation, respectively). Their absorption and emission properties are therefore expected to be qualitatively quite similar. This is confirmed by experimental data. The absorption maxima of these compounds are almost coincident, and the luminescence maxima, lifetimes, and quantum yields are also very similar (Table 2). As already discussed in detail elsewhere for **4t**^[14, 15] and **10t**,^[18] luminescence originates from the peripheral units, where the lowest-energy excited state (namely, $(bpy)_2Ru \rightarrow (\mu-2,3-dpp)$ CT) is localized. Efficient electronic energy transfer occurs from the inner (higher energy) units to the peripheral (lower energy) ones. On increasing the size of the dendrimers there is a strong increase in their ability to absorb sunlight (see ϵ values in Table 2), while the emission lifetimes and quantum yields are only slightly affected. This indicates that, with increasing size within this family of dendrimers, it is possible to obtain better antennas for light harvesting.

In the **4p** and **10p** "protected" dendrimers, the presence of methylated peripheral ligands causes strong modifications in the absorption and emission properties compared with those exhibited by the **bpy** analogues **4t** and **10t**. The peripheral Ru^{II} ions of **4p** and **10p** are more difficult to oxidize than the Ru^{II} ions carrying **bpy** as peripheral ligands (Table 1); as a consequence, the energy of the (peripheral ligand) $_2Ru \rightarrow (\mu-2,3-dpp)$ CT transition shifts to the blue region on moving from the "bpy" dendrimers to the "protected" ones. At the same time, the $Ru \rightarrow (2,3-Medpp^+)$ CT transition is expected to be at substantially lower energy than the corresponding $Ru \rightarrow bpy$ CT transition because of the different acceptor properties of **bpy** and **2,3-Medpp**⁺. The $Ru \rightarrow$ (peripheral ligand) and $Ru \rightarrow$ (bridging ligand) CT bands therefore tend to merge on going from **10t** to **10p**. Furthermore, "remote" charge transfer transitions involving the peripheral ligands are lowered in energy.^[131] The result of such a situation is a poorly resolved absorption spectrum for the "protected" dendrimers (Fig. 10).

A comparison of the properties of the "protected" dendrimers **4p** and **10p** (Table 2) shows that similarities within this family are not as great as for the analogous "bpy" dendrimers. Apparently, the introduction of additional charges and strong electron-withdrawing groups in the periphery of the supramolecular array increases the electronic interaction of the peripheral units with the neighboring units.

Since excited states involving different units are expected to lie close in energy, the assignment of the luminescence of **4p** and **10p** to specific metal-based units is not straightforward. It should be noted (Table 2) that, on going from fluid solution at 298 K to rigid matrix at 77 K, the emission maximum of **4p** is blue-shifted by only 300 cm^{-1} , whereas the blue shift shown by **4t**, whose emission certainly originates from the peripheral units, is much larger ($\approx 1400\text{ cm}^{-1}$). The shift of MLCT luminescence on going from rigid matrix to fluid solution is mainly due to solvent polarization effects.^[132] Such a solvent effect is expected to be much larger for peripheral units than for inner ones. Therefore, it seems reasonable to assign the luminescence of **4p** to a $Ru \rightarrow (\mu-2,3-dpp)$ CT excited state of the central unit. It should be noted, however, that in **4p** (as well as in **10p**) the electrochemical data suggest that the lowest MLCT excited state is a remote $Ru(\text{inner}) \rightarrow (2,3-Medpp^+)$ level. At present, we cannot say whether this level is involved in the luminescence process, but the small shift in the luminescence band on passing from fluid solution to rigid matrix would exclude this possibility. The longer luminescence lifetime and higher quantum yield of **4p** with respect to **4t** can, at least in part, be attributed to an energy-gap effect.^[133] In the case of **10p** the assignment of the

luminescent level can follow the same arguments discussed above for **4p**, although the situation is of course more complicated by the presence of intermediate units.

In the "deprotected" dendrimers **4d** and **10d**, interactions with the environment, which are also responsible for adsorption on electrodes (see above), can occur because of the presence of free chelating sites. Such interactions are probably responsible for the very weak or absent luminescence.

Extension to other metals and other ligands: The interest in highly branched polynuclear metal complexes, and more generally in dendritic species, is related not so much to their size, but rather to the presence of different components. An ordered array of different components can in fact generate valuable properties, such as the presence of cavities of different sizes, surfaces with specific functions, gradients for photoinduced directional energy and electron transfer, and sites for multielectron transfer catalysis. Our "complexes-as-metals and complexes-as-ligands" synthetic strategy is characterized by a *full, step-by-step control of the growth process*. Therefore we can choose the most appropriate building block at each step of the synthesis. For example, by reacting **1d** with **1't** or **3't** species containing different metals and/or ligands (e.g., Ru^{II} , Os^{II} **bpy**, **biq** (2,2'-biquinoline), **2,3-dpp**, and **2,5-dpp** (2,5-bis(2-pyridyl)pyrazine)), we have prepared nine tetranuclear^[14] and six decanuclear^[18] mixed-metal and/or mixed-ligand species. The same synthetic procedure can be applied to each **d**-type "complex ligand" of the successive generations (Fig. 4) to produce a multitude of higher nuclearity species where specific sites of the dendrimer are occupied by desired metals and/or ligands. The reported synthesis of the **22t** compound (Fig. 5) is an example of such a reaction on the first generation **4d**-dendrimer. Figure 13 shows a few of the many possible species that can be obtained starting from the **4d**-core. Besides the Ru^{II} and Os^{II} polypyridine complexes, other building blocks can be used, such as cyclometalated complexes of Rh^{III}

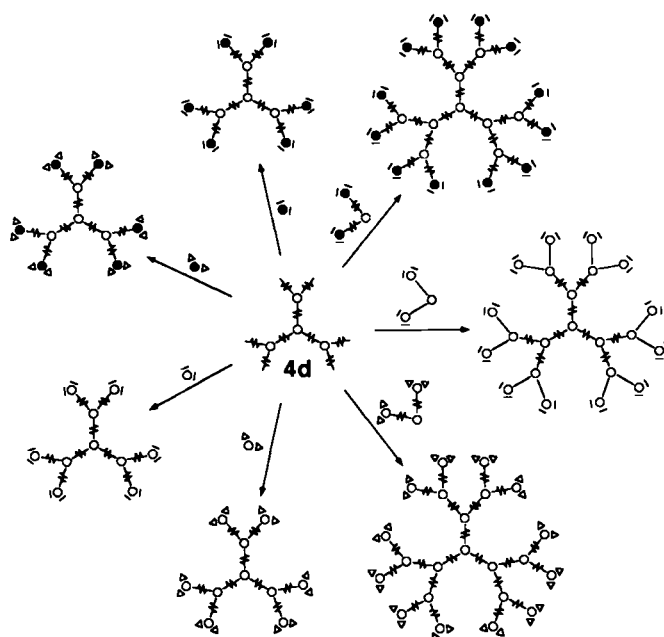


Fig. 13. In our synthetic approach, each deprotected (**d**) compound can be used as a core for convergent synthetic processes. This Figure shows schematically some of the compounds that have been [18] or can be obtained starting from the **4d** "complex ligand" core. Symbols: ●, Os^{2+} ; ○, $2,5-dpp$ bridging ligand; Δ, **biq** terminal ligand [18b]; the other symbols are explained in Figure 1. The two labile chloride ligands in the "complex metals" have been omitted for clarity.

and Ir^{III}. Tetranuclear compounds containing Ru/Rh, Ru/Ir, Os/Rh, and Os/Ir have already been prepared,^[7f, 34] and the design and synthesis of dendrimers based on three or more different metals are under way in our laboratories.

Conclusions

We have designed a divergent procedure, based on the “complexes-as-metals and complexes-as-ligands” synthetic strategy to prepare polynuclear metal complexes of nanometer size and dendritic structure. The key components (Fig. 2) are the 1d-core [Ru(2,3-dpp)₃]²⁺ (generation “zero”) and the 1p-building block, [Ru(2,3-Medpp⁺)₂Cl₂]²⁺, which contains two labile Cl[−] ions and two protected 2,3-dpp bridging ligands. Species with four, ten, and twenty-two metal centers have been prepared. They exhibit very intense absorption bands in the UV and visible spectral region, a MLCT luminescence both in rigid matrix at 77 K and in fluid solution at room temperature, and several oxidation (metal-based) and reduction (ligand-based) processes. The dendrimer with twenty-two metal atoms, which is one of the largest Werner-type complexes prepared so far, contains 1090 atoms, has a molecular weight of 10890 daltons, an approximate size of 5 nm, an absorption maximum at 542 nm with $\epsilon = 202000 \text{ M}^{-1} \text{ cm}^{-1}$, a luminescence band at 786 nm ($\tau = 45 \text{ ns}$ in fluid solution at room temperature), and a peak at +1.52 V (vs. SCE), which corresponds to the simultaneous oxidation of the twelve equivalent and weakly interacting peripheral metals. For the tetra- and decanuclear compounds, interesting differences have been observed in the absorption spectra, luminescence properties, and redox behavior for the species bearing protected 2,3-Medpp⁺, deprotected 2,3-dpp, or bpy ligands at their periphery.

Our dendrimers differ from most of those prepared so far for two fundamental reasons: 1) each building block exhibits valuable intrinsic properties such as absorption of visible (solar) light, luminescence, and oxidation and reduction levels at accessible potentials and 2) by a suitable choice of the building blocks, different metals and/or ligands can be placed in specific sites of the supramolecular array. In this way our dendrimers can incorporate many “pieces of information” and can therefore be used to perform valuable functions such as light harvesting, directional energy transfer, and exchange of a controlled number of electrons at a given potential.

Experimental Section

Materials and methods: The preparations of complexes [Ru(2,3-dpp)₃](PF₆)₂ [24] (**1d**), [Ru{(μ-2,3-dpp)Ru(bpy)₂}(PF₆)₃]₃ [14b, 15] (**4t**), [Ru{(μ-2,3-dpp)Ru(bpy)₂}(PF₆)₂Cl₂](PF₆)₄ [14c, 16a] (**3t**), [Ru{(μ-2,3-dpp)Ru{(μ-2,3-dpp)Ru(bpy)₂}(PF₆)₂Cl₂}(PF₆)₂₀] (**10t**), and the protected ligand (2,3-Medpp)(PF₆)₂ [23] have been previously reported. For infrared spectra (KBr pellets) a Perkin-Elmer 1330 spectrometer was used. Elemental analyses were obtained by a Carlo Erba 1106 apparatus. ¹H NMR spectra were performed by a Varian Gemini 200 MHz in CD₃CN solution. Absorption spectra were obtained in acetonitrile solution at room temperature by means of a Perkin-Elmer λ-6 spectrophotometer. Luminescence spectra were obtained with a Perkin-Elmer LS-50 spectrofluorimeter. Emission lifetimes were measured with an Edinburgh 199 single-photon counting equipment. Emission quantum yields were measured at room temperature (20 °C) with the optically dilute method [35] calibrating the spectrofluorimeter with a standard lamp. [Ru(bpy)₃]²⁺ in aerated aqueous solution was used as a quantum yield standard, assuming a value of 0.028 [36]. Electrochemical measurements were carried out in argon-purged acetonitrile solution at room temperature with a PAR 273 multipurpose equipment interfaced to a PC. The working electrode was a Pt microelectrode or a glassy carbon (8 mm², Amel) electrode. The counter-electrode was a Pt wire, and the reference electrode was a SCE separated with a fine glass frit. The concentration of the complexes was $3 \times 10^{-4} \text{ M}$. Tetraethylammonium hexafluorophosphate was

used as supporting electrolyte. Cyclic voltammograms were obtained at scan rates of 20, 50, and 200 mV s^{−1}. For reversible processes, half-wave potentials (vs. SCE) were calculated as an average of the cathodic and anodic peaks. The criteria for reversibility were the separation between cathodic and anodic peaks, the close to unity ratio of the intensities of the cathodic and anodic currents, and the constancy of the peak potential on changing scan rate. The number of exchanged electrons was measured with DPV experiments performed with a scan rate of 20 mV s^{−1}, a pulse height of 75 mV, and a duration of 40 ms. The procedure for the calibration of the number of electrons corresponding to the various redox waves has been described in detail [18b]. Experimental errors in the reported data are as follows: absorption maxima, 2 nm; emission maxima, 5 nm; emission lifetimes, 10%; emission quantum yields, 20%; redox potentials, 20 mV. As far as molar absorption coefficients are concerned, the uncertainty in their absolute values is $\approx 10\%$ because of the highly diluted solutions used (10^{-5} – 10^{-4} M).

[Ru(2,3-Medpp)₂Cl₂](PF₆)₂ (1p**):** A suspension of RuCl₃·3H₂O (0.050 g, 0.19 mmol), (2,3-Medpp)(PF₆) (0.158 g, 0.40 mmol), and LiCl (0.054 g, 1.27 mmol) in 1:2 (v/v) water/ethanol (18 mL) was refluxed for 4 h. The violet solution was cooled to room temperature, an excess of solid NH₄PF₆ was added, and the mixture was taken to dryness by rotary evaporation in vacuo. The residue was dissolved in acetonitrile and purified by flash chromatography on Sephadex G-10. By partial evaporation of the eluate, addition of diethyl ether, and filtration, a violet powder was recovered. Yield: 0.166 g (90%). Anal. calcd for C₃₀H₂₆F₁₂Cl₂N₄P₂Ru·H₂O: C, 36.8; H, 2.9; N, 11.4. Found: C, 36.7; H, 2.9; N, 11.3. Selected IR absorption maxima (cm^{−1}): $\tilde{\nu} = 1621 \text{ (m)}$, 1618 (sh, m), 1592 (w, br), 1560 (sh, w), 1550 (m), 1511 (m), 1513 (m), 1505 (sh, m), 1460 (m, br), 1448 (m), 1404 (s). ¹H NMR (CD₃CN): several singlets of different intensities between $\delta = 4.55$ and 4.05, attributable to the methyl protons of different isomers and blocked conformers. Conductivity (acetonitrile, approx. $1 \times 10^{-3} \text{ mol L}^{-1}$, 293 K): $\Lambda = 364 \Omega^{-1} \text{ mol}^{-1} \text{ cm}^2$.

[Ru{(μ-2,3-dpp)Ru(2,3-Medpp)₂}(PF₆)₄] (4p**):** The preparation and characterization of this compound was briefly reported in ref. [7b]. More details are given here. Silver nitrate (0.033 g, 0.192 mmol) was added to a suspension of **1p** (0.092 g, 0.096 mmol) in 1:2 (v/v) water/ethanol (9 mL), and the mixture stirred for 2 h at room temperature. Then **1d** (0.035 g, 0.032 mmol) was added and the mixture refluxed for 48 h. The mother liquor was cooled to room temperature, AgCl was separated by repeated centrifugation, and the solution was treated with an excess of solid NH₄PF₆. The red powder that formed was filtered off, dissolved in acetonitrile and purified by S. E. C. on Sephadex G-10. From the eluate the product was recovered as wine-red powder by addition of ethanol, partial evaporation in vacuo, and filtration. It was washed with small portions of cold ethanol, then with diethyl ether, and eventually dried in vacuo. Yield: 0.105 g (71%). Anal. calcd for C₁₃₂H₁₀₈F₈₄N₃₆P₁₂Ru₄·8H₂O: C, 33.2; H, 2.6; N, 10.6. Found: C, 32.6; H, 2.3; N, 10.6. Selected IR absorption maxima (cm^{−1}): $\tilde{\nu} = 1622 \text{ (m)}$, 1619 (sh, m), 1600 (w), 1581 (w), 1511 (m), 1505 (sh, m), 1465 (m), 1455 (w), 1410 (s). ¹H NMR (CD₃CN solution): several singlets of different intensities between $\delta = 4.20$ and 4.47, attributable to the methyl protons of different diastereoisomers and blocked conformers. Conductivity (acetonitrile, ca. $1 \times 10^{-3} \text{ mol L}^{-1}$, 293 K): $\Lambda = 875 \Omega^{-1} \text{ mol}^{-1} \text{ cm}^2$.

[Ru{(μ-2,3-dpp)Ru(2,3-dpp)₂}(PF₆)₆] (4d**):** The preparation and characterization of this compound has been briefly reported in ref. [7b]. More details are given here. A solution containing **4p** (0.085 g, 0.018 mmol) and a very large excess of 1,4-diazabicyclo[2.2.2]octane (DABCO) in dry acetonitrile (15 mL) was refluxed for 6 d. After cooling of the solution to room temperature and addition of ethanol, the reaction mixture was concentrated on a rotary evaporator until a substantial amount of precipitate was obtained. This was filtered off, dissolved in acetonitrile, and purified by flash chromatography on Sephadex G-15. On adding diethyl ether to the partially evaporated eluate, a violet powder resulted, which was filtered off and recrystallized from methanol in presence of NH₄PF₆. Yield: 0.040 g (60%). Anal. calcd for C₁₂₆H₉₀F₄₈N₃₆P₆Ru₄·2H₂O: C, 40.8; H, 2.8; N, 13.6. Found: C, 40.7; H, 2.5; N, 13.8. Selected IR absorption maxima (cm^{−1}): $\tilde{\nu} = 1590 \text{ (s, br)}$, 1560 (s), 1550 (s), 1540 (sh, m), 1505 (w, br), 1475 (m), 1462 (m), 1458 (sh, m), 1436 (m), 1412 (s), 1398 (sh, m), 990 (w). ¹H NMR (CD₃CN solution): no signals attributable to methyl groups. Conductivity (acetonitrile, ca. $1 \times 10^{-3} \text{ mol L}^{-1}$, 293 K): $\Lambda = 472 \Omega^{-1} \text{ mol}^{-1} \text{ cm}^2$.

[Ru{(μ-2,3-dpp)Ru{(μ-2,3-dpp)Ru(2,3-Medpp)₂}(PF₆)₂}(PF₆)₃₂] (10p**):** A suspension of **1p** (0.085 g, 0.089 mmol) in 1:2 (v/v) water/ethanol (8 mL) was treated with silver nitrate (0.030 g, 0.18 mmol). After 2 h of stirring at room temperature, **4d** (0.054 g, 0.015 mmol) was added and the mixture refluxed for 7 d. AgCl was removed by repeated centrifugations and an excess of solid NH₄PF₆ was added. The violet solid that formed was filtered off, dissolved in acetonitrile and purified by flash chromatography on Sephadex G-25. From the eluate the product was recovered by addition of ethanol and partial evaporation in vacuo. Yield: 0.110 g (70%). Anal. calcd for C₃₀₆H₂₄₀F₁₉₂N₈₄P₃₂Ru₁₀: C, 34.2; H, 2.3; N, 11.0. Found: C, 34.0; H, 2.4; N, 11.3. Selected IR absorption maxima (cm^{−1}): $\tilde{\nu} = 1623 \text{ (m)}$, 1620 (sh, m), 1602 (w), 1511 (m), 1509 (m), 1506 (sh, m), 1499 (w), 1466 (m), 1456 (w), 1411 (s). ¹H NMR (CD₃CN solution): several singlets of different intensities between $\delta = 4.15$ and 4.45, attributable to the methyl protons of different diastereoisomers

and blocked conformers. Conductivity (acetonitrile, ca. $1 \times 10^{-3} \text{ mol L}^{-1}$, 293 K): $\Lambda = 1983 \Omega^{-1} \text{ mol}^{-1} \text{ cm}^2$.

[Ru(μ -2,3-dpp)Ru(μ -2,3-dpp)Ru(μ -2,3-dpp) $_2$] $_3$ (PF $_6$) $_{20}$ (10d): The procedure for the deprotection of complex **10p** was analogous to that employed for **4p**. The reaction was performed on 0.060 g (0.006 mmol) of **10p** in acetonitrile (10 mL), using DABCO in a molar ratio of ca. 300:1, a reaction time of 8 d, and Sephadex G-25 for the purification. Yield: 0.035 g (66%). Anal. calcd for C $_{294}$ H $_{204}$ F $_{120}$ N $_{84}$ P $_{20}$ Ru $_{10}$: C, 40.0; H, 2.4; N, 13.3. Found: C, 39.9; H, 2.5; N, 13.1. Selected IR absorption maxima (cm $^{-1}$): $\tilde{\nu} = 1591$ (s, br), 1562 (s), 1551 (s), 1540 (sh, m), 1476 (m), 1464 (m), 1460 (sh, m), 1440 (m), 1415 (s), 1400 (sh, m), 990 (w). $^1\text{H NMR}$ (CD $_3$ CN solution): no signals attributable to methyl groups. Conductivity (acetonitrile, ca. $1 \times 10^{-3} \text{ mol L}^{-1}$, 293 K): $\Lambda = 1056 \Omega^{-1} \text{ mol}^{-1} \text{ cm}^2$.

[Ru(μ -2,3-dpp)Ru(μ -2,3-dpp)Ru(μ -2,3-dpp)Ru(bpy) $_2$] $_2$] $_3$ (PF $_6$) $_{44}$ (22t): The preparation and characterization of this compound was briefly reported in ref. [7b]. More details are given here. Compound **3t** (0.084 g, 0.042 mmol) in 1:1 (v/v) water/ethanol (5 mL) was treated with silver nitrate (0.014 g, 0.084 mmol). After the mixture had been stirred at room temperature for 2 h, a solution of **4d** (0.025 g, 0.007 mmol) in ethylene glycol (3 mL) was added. The reaction mixture was refluxed for 7 d, then cooled to room temperature. AgCl was separated by repeated centrifugations, the mother liquor concentrated by evaporation in vacuo, and an excess of solid NH $_4$ PF $_6$, methanol (2 mL) and diethyl ether (10 mL) were added. The crude product was filtered off and then purified by S. E. C. on Sephadex G-75 (acetonitrile eluant). The eluate was concentrated in vacuo to 2 mL, and the product **22t** was recovered as a cyclamen (very dark reddish purple) powder by addition of diethyl ether (about 15 mL). Yield: 0.086 g (73%) after purification. Anal. calcd including 25H $_2$ O: C, 36.2; H, 2.6; N, 10.0. Found: C, 35.9; H, 2.3; N, 10.4. Selected IR absorption maxima (cm $^{-1}$): $\tilde{\nu} = 1602$ (s), 1558 (w, br), 1465 (s), 1445 (s), 1419 (s), 1392 (s). $^1\text{H NMR}$ (CD $_3$ CN solution): no signals attributable to methyl groups. Conductivity (acetonitrile, ca. $1 \times 10^{-3} \text{ mol L}^{-1}$, 293 K): $\Lambda = 2297 \Omega^{-1} \text{ mol}^{-1} \text{ cm}^2$.

Reactivity toward methylation: A solution of [Ru(bpy) $_2$ (2,3-dpp)](PF $_6$) $_2$ (0.030 g, 0.032 mmol) in dry 1,2-dichloroethane (6 mL) was added under nitrogen to a suspension of (CH $_3$) $_3$ BOF $_4$ (0.006 g, 0.038 mmol) in the same solvent (6 mL). After refluxing for 45 min, the reaction mixture was cooled to room temperature and rotary evaporated to dryness. The residue was dissolved in acetonitrile, and a saturated solution of NH $_4$ PF $_6$ in ethanol was added. The mixture was concentrated on a rotary evaporator to induce the precipitation of the product. This was filtered off, washed with small amounts of ethanol and diethyl ether, and dried in vacuo. Yield: 0.028 g (80%). $^1\text{H NMR}$ (CD $_3$ CN solution): two singlets at $\delta = 4.20$ and 3.93 attributable to the methyl protons of two different isomers. The same experimental procedure was used to test the reactivity toward methylation of the other compounds.

Acknowledgments. We wish to thank G. Gubellini, L. Minghetti, M. Minghetti, L. Ventura, and F. Stillitano for technical assistance. This work was supported by Consiglio Nazionale delle Ricerche (Progetto Strategico Tecnologie Chimiche Innovative), and Ministero dell'Università e della Ricerca Scientifica e Tecnologica. S. C., G. D., and S. S. would like to thank NATO for the research grant No. 920609 (Supramolecular Chemistry), and S. S. would also like to thank CNR for the grant No. 201.03.20.

Received: November 21, 1994 [F20]

- [1] For some very recent papers, see: a) M. A. Coffin, M. R. Bryce, A. S. Batanov, J. A. K. Howard, *J. Chem. Soc. Chem. Commun.* **1993**, 552; b) A. W. van der Made, P. W. N. M. van Leeuwen, J. de Wilde, R. A. C. Brandes, *Adv. Mater.* **1993**, 5, 466; c) R. Mülhaupt, C. Wörner, *Angew. Chem. Int. Ed. Engl.* **1993**, 32, 1306; d) E. M. M. de Brabander-van den Berg, E. W. Meijer, *Angew. Chem. Int. Ed. Engl.* **1993**, 32, 1308; e) Z. Xu, J. S. Moore, *Angew. Chem. Int. Ed. Engl.* **1993**, 32, 1354; f) F. Moulines, L. Djakovitch, R. Boese, B. Gloaguen, W. Thiel, J.-L. Fillaut, M.-H. Delville, D. Astruc, *Angew. Chem. Int. Ed. Engl.* **1993**, 32, 1075; g) G. R. Newkome, C. N. Moorefield, J. M. Keith, G. R. Baker, G. H. Escamilla, *Angew. Chem. Int. Ed. Engl.* **1994**, 33, 666; h) C. J. Hawker, K. L. Wooley, J. M. J. Fréchet, *J. Chem. Soc. Chem. Commun.* **1994**, 925; i) T. Nagasaki, O. Kimura, M. Ukon, S. Arimori, I. Hamachi, S. Shinkai, *J. Chem. Soc. Perkin Trans. 1* **1994**, 75; j) K. Kadei, R. Moors, F. Vögtle, *Chem. Ber.* **1994**, 127, 897; k) P. J. Dandlinker, F. Diederich, M. Gross, C. B. Knobler, A. Louati, E. M. Sandford, *Angew. Chem. Int. Ed. Engl.* **1994**, 33, 1739.
- [2] E. Buchlein, W. Wehner, F. Vögtle, *Synthesis* **1978**, 155.
- [3] G. R. Newkome, Z. Yao, G. R. Baker, V. K. Gupta, *J. Org. Chem.* **1985**, 50, 2003.
- [4] D. A. Tomalia, H. Baker, J. R. Dewald, M. Hall, G. Kallos, S. Martin, J. Roeck, J. Ryder, P. Smith, *Polymer J.* **1985**, 17, 117.
- [5] a) D. A. Tomalia, A. M. Naylor, W. A. Goddard III, *Angew. Chem. Int. Ed. Engl.* **1990**, 29, 138; b) G. R. Newkome, C. N. Moorefield, G. R. Baker, *Aldrichimica Acta* **1992**, 25, 31; c) D. A. Tomalia, H. D. Durst, *Topics Curr. Chem.* **1993**, 165, 193; d) J. M. J. Fréchet, *Science* **1994**, 263, 1710.
- [6] a) H.-B. Meckelburger, W. Jaworek, F. Vögtle, *Angew. Chem. Int. Ed. Engl.* **1992**, 31, 1571; b) R. Dagani, *Chem. Eng. News* **1993**, February 1, 28; c) M. A. Fox, W. E. Jones Jr., D. M. Watkins, *Chem. Eng. News* **1993**, March 15, 38; d) D. A. O'Sullivan, *Chem. Eng. News* **1993**, August 16, 20; e) P. Hodge, *Nature* **1993**, 362, 18.
- [7] a) G. Denti, S. Serroni, S. Campagna, A. Juris, M. Ciano, V. Balzani in *Perspectives in Coordination Chemistry* (Eds.: A. F. Williams, C. Floriani, A. E. Merbach), VCH, Basel, **1992**, p. 153; b) S. Serroni, G. Denti, S. Campagna, A. Juris, M. Ciano, V. Balzani, *Angew. Chem. Int. Ed. Engl.* **1992**, 31, 1493; c) G. Denti, S. Serroni, S. Campagna, A. Juris, V. Balzani, *Molec. Cryst. Liquid Cryst.* **1993**, 234, 79; d) G. Denti, S. Campagna, V. Balzani in *Mesomolecules: from Molecules to Materials* (Eds.: D. Mendenhall, A. Greenberg, J. Lieberman), Chapman and Hall, New York, **1994**, p. 69; e) V. Balzani, G. Denti, S. Serroni, S. Campagna, V. Ricevuto, A. Juris, *Indian Acad. Sciences* **1993**, 105, 1; f) V. Balzani, S. Campagna, G. Denti, A. Juris, S. Serroni, M. Venturi, *Coord. Chem. Rev.* **1994**, 132, 1.
- [8] *Molecular Electronics Devices* (Eds.: F. L. Carter, R. E. Siatkowski, H. Wohltjen), North-Holland, Amsterdam, **1988**.
- [9] V. Balzani, L. Moggi, F. Scandola in *Supramolecular Photochemistry* (Ed.: V. Balzani), Reidel, Dordrecht, The Netherlands, **1987**, p. 1.
- [10] J.-M. Lehn, *Angew. Chem. Int. Ed. Engl.* **1990**, 29, 1304.
- [11] V. Balzani, F. Scandola, *Supramolecular Photochemistry* Horwood, Chichester, U. K., **1991**.
- [12] a) R. Amadelli, R. Argazzi, C. A. Bignozzi, F. Scandola, *J. Am. Chem. Soc.* **1990**, 112, 7099; b) B. O'Regan, M. Graetzel, *Nature* **1991**, 353, 737.
- [13] a) A. Juris, V. Balzani, F. Barigelletti, S. Campagna, P. Belser, A. von Zelewsky, *Coord. Chem. Rev.* **1988**, 84, 85; b) T. J. Meyer, *Acc. Chem. Res.* **1989**, 22, 163; c) F. Scandola, M. T. Indelli, C. Chiorboli, C. A. Bignozzi, *Photochem. Rev.* **1990**, 158, 73; d) K. Kalyanasundaram, *Photochemistry of Polypyridine and Porphyrin Complexes*, Academic Press, London, **1991**.
- [14] a) S. Campagna, G. Denti, L. Sabatino, S. Serroni, M. Ciano, V. Balzani, *J. Chem. Soc. Chem. Commun.* **1989**, 1500; b) G. Denti, S. Campagna, L. Sabatino, S. Serroni, M. Ciano, V. Balzani, *Inorg. Chem.* **1990**, 29, 4750; c) G. Denti, S. Serroni, S. Campagna, V. Ricevuto, V. Balzani, *Inorg. Chim. Acta* **1991**, 182, 127; d) G. Denti, S. Serroni, S. Campagna, V. Ricevuto, V. Balzani, *Coord. Chem. Rev.* **1991**, 111, 227.
- [15] The first tetranuclear complex was prepared by W. R. Murphy Jr., K. J. Brewer, G. Gettcliffe, J. D. Petersen, *Inorg. Chem.* **1989**, 28, 81.
- [16] a) S. Campagna, G. Denti, S. Serroni, M. Ciano, V. Balzani, *Inorg. Chem.* **1991**, 30, 3728; b) G. Denti, S. Serroni, S. Campagna, V. Ricevuto, A. Juris, V. Balzani, *Inorg. Chim. Acta* **1992**, 198–200, 507.
- [17] G. Denti, S. Campagna, L. Sabatino, S. Serroni, M. Ciano, V. Balzani, *Inorg. Chim. Acta* **1990**, 176, 175.
- [18] a) S. Serroni, G. Denti, S. Campagna, M. Ciano, V. Balzani, *J. Chem. Soc. Chem. Commun.* **1991**, 944; b) G. Denti, S. Campagna, S. Serroni, M. Ciano, V. Balzani, *J. Am. Chem. Soc.* **1992**, 114, 2944.
- [19] S. Campagna, G. Denti, S. Serroni, M. Ciano, A. Juris, V. Balzani, *Inorg. Chem.* **1992**, 31, 2982.
- [20] a) G. R. Newkome, F. Cardullo, E. C. Constable, C. N. Moorefield, A. M. W. Cargill Thompson, *J. Chem. Soc. Chem. Commun.* **1993**, 925; b) Y.-H. Liao, J. R. Moss, *J. Chem. Soc. Chem. Commun.* **1993**, 1774; c) S. Achar, R. J. Puddephatt, *Angew. Chem. Int. Ed. Engl.* **1994**, 33, 847; d) G. R. Newkome, C. N. Moorefield, *Macromol. Symp.* **1994**, 77, 63.
- [21] For a preliminary communication, see ref. [7b].
- [22] For some relevant, recent papers on the electrochemical and photophysical properties of Ru II complexes containing the 2,3-dpp-bridged ligand, see: a) J. B. Cooper, D. B. MacQueen, J. D. Petersen, D. W. Wertz, *Inorg. Chem.* **1990**, 29, 3701; b) K. Kalyanasundaram, M. Graetzel, Md. K. Nazeeruddin, *J. Phys. Chem.* **1992**, 96, 5865; c) J. E. B. Johnson, R. L. Ruminski, *Inorg. Chim. Acta* **1993**, 208, 231; d) J. S. Bridgewater, L. M. Vogler, S. M. Molnar, K. J. Brewer, *Inorg. Chim. Acta* **1993**, 208, 179; e) M. M. Richter, K. J. Brewer, *Inorg. Chem.* **1993**, 32, 2827; f) S. Roffia, M. Marcaccio, C. Paradisi, F. Paolucci, V. Balzani, G. Denti, S. Serroni, S. Campagna, *Inorg. Chem.* **1993**, 32, 3003.
- [23] S. Serroni, G. Denti, *Inorg. Chem.* **1992**, 31, 4251 and references therein.
- [24] K. J. Brewer, W. R. Murphy Jr., S. R. Spurlin, J. D. Petersen, *Inorg. Chem.* **1986**, 25, 882.
- [25] That is, a species containing twenty-two metal ions; see P. B. Block, W. H. Powell, W. C. Fernelius, *Inorganic Chemical Nomenclature*, American Chemical Society, Washington, D. C., **1990**.
- [26] G. Denti, S. Serroni, G. Sindona, N. Uccella, *J. Am. Soc. Mass Spectrom.* **1993**, 4, 306.
- [27] G. Predieri, C. Vignali, G. Denti, S. Serroni, *Inorg. Chim. Acta* **1993**, 205, 145.
- [28] See, for example, R. Hage, A. H. J. Dijkhnis, J. G. Haasnoot, R. Prins, J. Reedijk, B. E. Buchanan, J. G. Vos, *Inorg. Chem.* **1988**, 27, 2185.
- [29] a) G. Denti, S. Campagna, L. Sabatino, S. Serroni, M. Ciano, V. Balzani, in *Photochemical Conversion and Storage of Solar Energy* (Eds.: E. Pelizzetti, M. Schiavello), Kluwer, Dordrecht, Holland, **1991**, p. 27; b) V. Balzani, S. Campagna, G. Denti, S. Serroni, in *Photoprocesses in Transition Metal Complexes, Biosystems, and other Molecules: Experimental and Theory* (Ed.: E. Kochanski), Kluwer, Dordrecht, Holland, **1992**, p. 233.

- [30] In **10p**, oxidation of the central and of the three intermediate metal ions is expected to occur almost at the same potential. Therefore, it could be that oxidation first concerns the central metal ion, and that subsequent oxidation leads (by intramolecular electron transfer) to the formation of the three intermediate, almost not interacting, oxidized units.
- [31] Proximate $\text{Ru} \rightarrow \text{bpy}$ and $\text{Ru} \rightarrow (\mu\text{-}2,3\text{-dpp})$ excited states are stabilized by electrostatic interaction compared to remote CT excited states of the same orbital origin. This, however, is not the case for $\text{Ru} \rightarrow (2,3\text{-Medpp}^+)$ because the CT transition does not yield a negatively charged ligand.
- [32] Stabilization of the excited state by solvent repolarization cannot occur in a rigid matrix. See, for example: F. Barigelletti, A. Juris, V. Balzani, P. Belser, A. von Zelewsky, *J. Phys. Chem.* **1987**, *91*, 1095 and references therein.
- [33] J. V. Caspar, T. J. Meyer, *J. Am. Chem. Soc.* **1983**, *105*, 5583.
- [34] S. Serroni, A. Juris, S. Campagna, M. Venturi, G. Denti, V. Balzani, *J. Am. Chem. Soc.* **1994**, *116*, 9086.
- [35] J. N. Demas, G. A. Crosby, *J. Phys. Chem.* **1971**, *75*, 991.
- [36] K. Nakamaru, *Bull. Chem. Soc. Jpn.* **1982**, *55*, 2697.

VCH on Internet

Information
available on:

Books

Journals

Nonbooks

Electronic Products

www.vchgroup.de

VCH 